Journal of Non-Crystalline Solids 111 (1989) 48–54
North-Holland, Amsterdam

SPINNABILITY OF SILICA SOLS
Structural and rheological criteria

C.J. BRINKER and R.A. ASSINK
Sandia National Laboratories, Albuquerque, NM 87185–5800, USA

Received 16 February 1989
Revised manuscript received 8 May 1989

^{29}Si NMR spectroscopy of concentrated silicate sols, prepared by acid-catalyzed hydrolysis of TEOS in ethanol with H_2O/Si ratios, $r = 1.5$ or 1.7, followed by alcohol evaporation, shows that the polysilicate species responsible for spinnability are not simple rigid-rod, ladder polymers or linear polymers. Instead a distribution of silicate species is observed consistent with the products of a statistical (random) growth process. The primary criterion for spinnability is high viscosity without premature gelation. This is accomplished under acid-catalyzed conditions with low values of r.

1. Introduction

A fluid is spinnable if it is capable of assuming large irreversible deformations when subjected to uniaxial stress, a measure of spinnability being the maximum attainable elongation [1]. Experimental data show that spinnability is exhibited by materials differing greatly in structure and composition. Long fluid threads can be obtained from mineral oils, soap solutions, and honey as well as from polymer melts and inorganic sols. The maximum length of the fluid thread, x^*, depends on the material involved and the processing conditions. Generally for low viscosities, η, and low elongational velocities, V, x^* increases with the product, ηV, while a decrease in x^* is observed at very high values of ηV [1]. Two mechanisms are proposed to account for the breakage of fluid threads, cohesive failure and capillary wave instability (droplet formation). The former mechanism is most important at high ηV, conditions where viscoelastic fluids behave elastically. Capillary wave instability is most important at low viscosity, and is exacerbated by high surface tensions [1].

Several groups have investigated the rheological behavior of silicate sols prepared from tetraethylorthosilicate (TEOS) in order to establish the criteria for spinnability. Sacks and Sheu [2] observed that for acid-catalyzed systems prepared with H_2O/Si ratios, $r = 1$ or 2, the best spinnability occurred in viscous systems ($\eta > 100$ mPa-s) that were highly shear thinning but not thixotropic. Sakka et al. [3–6] evaluated acid- and base-catalyzed systems prepared with r values ranging from 1 to 20 by determining the concentration dependence of the reduced viscosity, η_{sp}/C:

$$\eta_{sp}/C = k_1/\rho \tag{1}$$

or

$$\eta_{sp}/C = [\eta] + k_2[\eta]^2 C, \tag{2}$$

where η_{sp} is the specific viscosity, C is concentration, k_1 and k_2 are constants, and ρ is density, and the molecular weight dependence of the intrinsic viscosity, $[\eta]$:

$$[\eta] = k_3 M_n^{\alpha}, \tag{3}$$

where M_n is the number average molecular weight, k_3 is a constant that depends on the polymer, solvent, and temperature, and α is an exponent that ranges from 0 to 2 depending on polymer structure.

Equation (1), which shows no concentration dependence of the reduced viscosity, pertains to systems composed of discrete, non-interacting

0022-3093/89/$03.50

polymers or particles [7]. Equation (2) pertains to extended, chain-like or linear polymers that exhibit a concentration dependence of η_{sp}/C [8]. Sakka and Kamiya [3] observed that, for an acid-catalyzed system prepared with $r = 1$, aging in open containers caused a progressively greater dependence of η_{sp}/C on C and eventually resulted in spinnability. This suggests that, for these conditions, solvent evaporation accompanied by continued hydrolysis and condensation causes a gradual progression of the silicate structure from small non-interacting species to extended, weakly-branched polymers responsible for spinnability. Base-catalyzed conditions as well as acid-catalyzed conditions with $r = 20$ exhibited no concentration dependence of η_{sp}/C and no evidence of spinnability [3].

It is postulated that the value of α in eq. (3) depends on the polymer or particle structure: $\alpha = 0$ for rigid, spherical particles, $\alpha = 0.5$ to 1.0 for flexible, chain-like or linear polymers, and $\alpha = 1.0$ to 2.0 for non-flexible or rigid rod polymers [9]. For example, $\alpha = 0.5$ for linear polydimethylsiloxane, $\alpha = 0.21$ to 0.28 for branched or crosslinked polymethylsiloxane, and $\alpha = 0.3$ for spherical polysilicates [8]. Sakka et al. observed that for acid-catalyzed silicate systems prepared with r values ranging from 1 to 20, α decreased with r (see table 1). Spinnability was observed only for α values above 0.5 corresponding to linear or perhaps rigid rod polymers [10].

In a subsequent study Sakka et al. explored fiber formation in silicate systems prepared from methyltriethoxysilane (MTES) or dimethyldiethoxysilane (DMES) [11]. They observed that the hydrolysis of DMES resulted preferentially in the formation of cyclic tetramers. Based on this observation it was suggested that rigid rod polymers, such as ladder polymers, are necessary for spinnability since linear polymers would tend to cyclize [11]. Ladder polymers have also been associated with the inflection in the viscosity versus time behavior observed in spinnable systems hydrolyzed with $r = 1.7$, which is close to the theoretical value required to form ladder polymers, viz 1.666. Various linear or ladder-like structures proposed by Kamiya et al. [12] to account for spinnability are shown below:

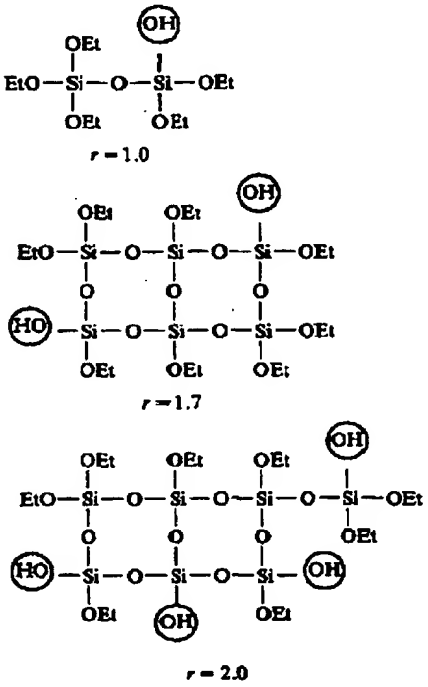

(4)

Table 1
The exponents α's for the alkoxide polymers and properties of $Si(OC_2H_5)_4$ solution

Solution	H_2O (r)	α	Type of polymer	Spinnability
1	1.0	0.75	linear	yes
2	2.0	0.64	linear	yes
3	5.0	0.5	branched	no
		0.2	three-dimensional	
4	20.0	0.34	three-dimensional spherical	no

In an attempt to understand the relationship between polymer structure and spinnability, we have used ^{29}Si NMR to examine the local chemical environment of Si in spinnable silicate systems. At least for the relatively high molecular weight systems used for fiber formation, knowledge of the average number of bridging and termi-

nal groups surrounding the central silicon [1] allows us to distinguish between several of the structures proposed to account for spinnability: linear polymers (Q^2), double chain ladder polymers (Q^3) and triple chain ladder polymers ($Q^3 : Q^4 = 2:1$).

2. Experimental

2.1. Materials

Spinnable silicate sols were prepared by two methods: (1) acid-catalyzed hydrolysis of TEOS in ethanol under reflux (mole ratios of TEOS: ethanol : H_2O : HCl = 1 : 3 : 1.5 : 0.0007) followed by ethanol distillation at 85°C under Ar and exposure to 100% RH water vapor at 80°C for 2–3 h, or (2) acid-catalyzed hydrolysis of TEOS in ethanol ($r = 1.7$) at 30°C followed by solvent evaporation at 80°C in an uncovered vessel according to the procedure of Sakka and coworkers [5–7].

Although in the first procedure virtually all the added alcohol and alcohol produced by hydrolysis and condensation was removed by distillation under Ar, spinnability [2] was not observed at the end of the distillation process. Therefore some additional hydrolysis appears necessary.

2.2. Instrumentation

The ^{29}Si NMR spectra were recorded at 39.6 MHz on a spectrometer described previously [13]. Broadband ^{1}H decoupling was applied only during acquisition in order to suppress the nuclear Overhauser effect and the RIDE pulse sequence [14] was used to reduce baseline roll. The pulse delay time was 45 s. Quantitatively similar spectra were obtained when chromium acetylacetonate, a spin relaxation agent, was added to the solution.

Preliminary small-angle X-ray scattering data were obtained on the spinnable system at full concentration and after dilutions by factors of 10, 100, or 1000 with anhydrous ethanol.

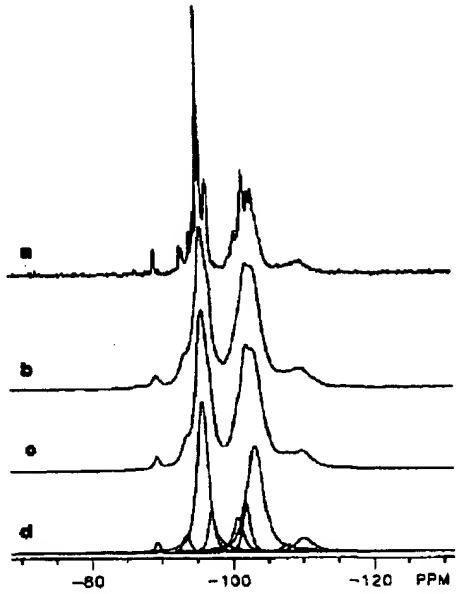

Fig. 1. Experimental and simulated ^{29}Si NMR spectra of the $H_2O = Si = 1.5$ spinnable sol–gel solution: (a) experimental, 1.0 Hz exponential line broadening; (b) experimental, 30 Hz exponential line broadening; (c) computer simulation; (d) resonance components of computer simulation.

3. Results and discussion

3.1. ^{29}Si NMR

The ^{29}Si NMR spectra of the spinnable sol–gel solutions are shown in figs. 1(a) and 2(a). The spectra exhibit resonances in four regions: Q^1 species, −82 to −90 ppm; Q^2 species, −91 to −99 ppm; Q^3 species, −99 to −106 ppm; and Q^4 species −106 to −112 ppm. The presence of Q^0 species (monomers as TEOS or in a hydrolyzed state) at or downfield from −82 ppm could not be detected. The assignment of sol–gel silicates into these regions has been discussed previously [16], and should be quite exact except for the downfield shift of resonances of highly strained species such as tricyclics. Significant quantities of

[1] In Q^n terminology, the n refers to the number of bridging oxygens (0–4) surrounding the central silicon atom.

[2] Spinnability was evaluated qualitatively by determining whether fibers could be drawn from the sol using a glass rod.

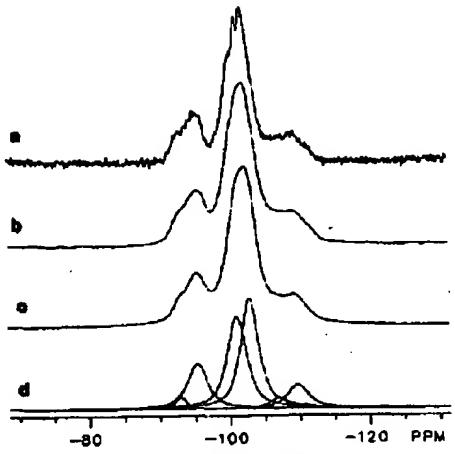

Fig. 2. Experimental and simulated ^{29}Si NMR spectra of the $H_2O = Si = 1.7$ spinnable sol–gel solution: (a) experimental, 1.0 Hz exponential line broadening; (b) experimental, 30 Hz exponential line broadening; (c) computer simulation; (d) resonance components of computer simulation.

such highly strained species are not expected to form under the present reaction conditions [17].

The spectra could not be accurately integrated into their resonance components directly because of the amount of overlap between resonances, particularly the Q^3 and Q^4 resonances. Therefore, simulation of the spectra by the General Electric 1280 software was used to determine the relative intensities of the resonances. The free induction decay was multiplied by a 30 Hz exponential function before Fourier transformation. The broadened spectra, shown in figs. 1(b) and 2(b), contain substantially fewer resonances which simplifies the simulation procedure without affecting the resultant areas of the various regions. Figures 1(c) and 2(c) show the simulated spectra while figs. 1(d) and 2(d) show the component resonances of the simulated spectra, for the two samples. The component resonances contain 70% Lorenztian and 30% Gaussian character. The simulation parameters were varied by trial and error to give the best visual fit of the experimental spectra. The relative areas of the simulated Q^n regions were reproducible to within $\pm 1.0\%$.

The relative areas of each of the Q^n regions determined by the simulation procedure are shown in the first column of table 2. The broad distribution of silicon functionalities indicates that the silicate polymers are not composed of any one of the simple repeat units shown in, (4): linear polymers (Q^2) or ladder polymers (Q^3 or $2Q^3:1Q^4$). The presence of significant amounts of Q^2, Q^3, and Q^4 species, and the many resonances evident within each of these spectral regions (figs. 1(a) and 2(a)) indicate that the polymers are very complex and highly branched.

The distributions shown in table 2 are reminiscent of the distributions seen for the equilibrium structure of tetramethoxysilane (TMOS) reacted with limited amounts of water [18]. These experimental distributions could be predicted quite accurately by a statistical reaction model [15] that assumes that all the hydrolysis and condensation rate constants depend only on the functional group reactivity, not the local silicon environment. The predictions of this model for $r = 1.5$ and $r = 1.7$ are shown in column 2 of table 2. The distributions predicted by the statistical reaction model differ qualitatively from the experimental distributions in two respects. First, the distributions predicted by the statistical reaction model are biased to higher functionalities compared to the

Table 2
The experimental and theoretical function distributions for the sol–gel silicon atom

Speciation	Experimental distribution	Theoretical distribution		
		$H_2O = 1.5$	$H_2O = 1.31$	$H_2O = 1.31$ $R = 0.35$
Q^0	0.0	0.4	1.4	0.0
Q^1	1.0	4.7	10.8	0.8
Q^2	41.9	21.1	30.6	41.5
Q^3	50.3	42.2	38.8	52.5
Q^4	6.8	31.6	18.4	5.2
Standard deviation		7.5	4.9	0.6
		$H_2O = 1.7$	$H_2O = 1.47$	$H_2O = 1.47$ $R = 0.35$
Q^0	0.0	0.0	0.5	0.0
Q^1	0.0	1.1	5.4	0.0
Q^2	18.3	9.7	22.8	19.5
Q^3	69.0	36.9	42.2	67.0
Q^4	12.7	52.2	29.2	13.5
Standard deviation		11.5	7.2	0.6

experimental distributions. Second, the distribution of the Q^n species predicted by the statistical reaction model are broader than the experimental distributions.

The bias to higher functionalities predicted by the statistical reaction model is a consequence of the incomplete reaction of the sol–gel system at the time when the NMR spectra were recorded. The moles of H_2O per mole of silicon consumed by condensation reactions can be calculated as follows:

$$\text{moles } H_2O = \tfrac{1}{2}Q^1 + Q^2 + \tfrac{3}{2}Q^3 + 2Q^4. \quad (5)$$

From the experimentally determined Q^n distributions of the sol-gel silicons, the moles of H_2O per mole of silicon that were consumed by condensation reactions are calculated to be 1.31 and 1.47 for the two samples. The remaining moles of H_2O per mole of silicon (0.19 for the first sample and 0.23 for the second plus any additional water supplied by the subsequent exposure to water vapor) were probably used to hydrolyze ethoxy groups, but the resultant silanols had not yet undergone condensation reactions. If the values of 1.31 and 1.47 moles of H_2O per mole of silicon are used in the statistical reaction model, the distributions shown in column 3 of table 2 are obtained. The calculated distributions now reflect the same degree of overall condensation as the sol–gel, but are still broader than the experimental distribution.

A trend to a narrower distribution can be explained if the early reactions are faster than average and the late reactions are slower than average. For example, suppose that the Q^0 to Q^1 reaction is very fast and that the Q^3 to Q^4 reaction is very slow. Then, the concentrations of both the Q^0 and Q^4 species will be diminished. Column 4 of table 2 shows the distribution calculated by a model which incorporates these ideas. The rate of the Q^0 to Q^1 was set equal to 1 and the rate of each successive reaction was then multiplied by a factor R, where R is less than 1. Thus the relative rate of Q^1 to Q^2 is R, the relative rate of Q^2 to Q^3 is R^2 and the relative rate of reaction of Q^3 to Q^4 is R^3. The value of R was then adjusted to minimize the standard deviation between the theoretical and experimental distributions. The best agreement between theory and experimental for the samples was obtained for $R = 0.35$. The standard deviations between the experimental distribution and the various model distributions are also shown in table 2. Obviously, the best prediction is generated by the model incorporating R, whose fit is well within the uncertainty of the experimentally determined distribution. A decreasing rate of condensation of a silicon atom as its state of condensation increases is reasonable on the basis of steric and inductive considerations [6]. Experiments have also shown that the condensation rate of dimeric species is much slower than the condensation rate of monomeric species in the TMOS sol–gel system [19].

Based on the above discussion, the sol–gel polymer in its spinnable state is a combination of silicon atoms forming linear segments, trifunctional branching points, and tetrafunctional branching points. It does not consist of simple, high molecular weight linear polymers (Q^2), double-chain ladder polymers (Q^3), or triple-chain ladder polymers ($Q^3 : Q^4 = 2:1$). Instead the distribution of silicon atoms among these various functionalities can be explained by very simple statistical arguments implying random, not ordered, growth processes.

3.2. Rheology and scattering

In addition to the local chemical structure, several other factors argue against the presence of rigid rod polymers in spinnable silicate sols. According to eq. (3), the exponent, α, is required to be 1–2 for rigid polymers, yet the largest value observed was 0.75. In order to give structural significance to the value of α, eq. (3) may be re-expressed in terms of a mass fractal dimension, D [20]:

$$\eta \sim R_g^3/M_n \sim k_4 M_n^{(3/D)-1}, \quad (6)$$

where R_g is the radius of gyration and k_4 is a constant. Since the mass fractal dimension of a rod is 1, eq. (6) predicts that for rigid-rod polymers $\alpha = (3/1) - 1 = 2$. According to eq. (6), $\alpha = 0.75$ corresponds to $D = 1.83$, a value in between that of a linear swollen polymer (self-avoiding random walk), $D = 5/3$, and either an ideal (ran-

dom walk) linear polymer or swollen branched polymer or reaction-limited cluster–cluster aggregate, $D \approx 2$ [21].

Although it is often possible to determine the value of D from small-angle scattering according to

$$I(K) \sim K^{-D} \quad (7)$$

a preliminary SAXS investigation of the spinnable system did not show a linear dependence of I on K. Instead the slit-smeared slopes increased progressively from $< 1/3$ to > 1 (corresponding approximately to $D < 1.33$ to $D > 2$) over the range $K = 0.01$ to 1. These curvature effects are generally attributed to strong polydispersity disallowing an interpretation of the slope according to eq. (7). Even though a fractal dimension describing the spinnable system has not been obtained, the preliminary SAXS data do not support $D = 1$, as expected for rigid-rod polymers.

3.3. Criterion for spinnability

From the combined results summarized above, we see that the criterion for spinnability is high viscosity of the sol without premature gelation. This criterion is achieved using acid catalysts and low values of r (generally < 2).

As discussed in the Introduction, for low elongational velocities, $\dot{V}$ (normally case for laboratory experiments), high viscosity is necessary to stabilize the fiber from capillary wave instabilities (droplet formation). Equations (2, 3, 6) indicate that for any particular concentration or extent of condensation (M_n), less-highly branched "extended" structures, e.g., chains or randomly branched polymers ($D \ll 3$), are more efficient than compact structures, e.g, discrete particles ($D = 3$), at increasing the viscosity. Extended structures interact at low concentrations and at low extents of condensation which explains the concentration and molecular weight dependence of the reduced and intrinsic viscosities, respectively. Although rigid-rod polymers ($D = 1$) confer the greatest effect on the viscosity per unit concentration or molecular weight, our NMR results clearly show that neither rod polymers nor linear polymers are necessary for spinnability.

However, high viscosity alone is not a sufficient condition for fiber formation. All gel forming systems by definition attain high viscosities, but most often the spinnable state is too short-lived to be of any practical consequence. Acid catalysts and low r values facilitate high viscosity without premature gelation.

Acid catalysts generally lead to extended structures as opposed to compact structures by promoting random (statistical) cluster–cluster growth that proceeds more or less irreversibly, i.e., without much rearrangement [22]. In addition sufficient acid concentrations to yield an effective pH near 2 minimize the condensation rate. This allows the viscosity to be increased by increasing the concentration (eq. 2) without causing immediate gelation. Kozuka et al. [23] found that for an acid-catalyzed TEOS system prepared with $r = 2$ spinnability was observed only when the viscosity was increased by solvent removal in an open container. In closed containers equivalent viscosities can be achieved only be continued condensation reactions leading to network formation and premature gelation.

Because ether (ROR) forming condensation reactions do not occur at low temperature, low H_2O/Si ratios, r, effectively reduce the functionality of Si, thereby promoting the formation of extended rather than compact structures. In addition, since OR terminated polymers do not react, the viscosity can increase via solvent removal as opposed to network formation leading to spinnability as described above.

An r value of 1 is theoretically sufficient to produce infinite chains, while r values of 1.66 and 2 are theoretically sufficient to produce double chain ladder polymers and fully condensed silica, respectively. However, in this study ($r = 1.5$ or 1.7) even reflux conditions followed by distillation of ethanol at 85°C did not drive the reaction to completion. Thus the system retains some uncondensed OH groups that may be important with regard to spinnability. Clearly in our experiments some hydrolysis of the terminal groups appears necessary, since solvent removal alone at 85°C in the absence of water vapor ($r = 1.5$) did not result in spinnable systems, whereas spinnability was observed after subsequent exposure of the sol to

100% RH water vapor at 80°C (conditions under which little further evaporation occurs). In all of the referenced work cited in this paper spinnability was achieved by aging the sols uncovered in uncontrolled environments, so that some amount of additional hydrolysis occurs during the concentration step. These hydrolyzed groups as well as additional silanol groups formed during fiber formation may be necessary to stabilize the drawn fiber. Sacks and Sheu for example found that although a sol prepared with $r = 1$ was spinnable, the drawn fibers were unstable toward droplet formation [2].

4. Conclusions

^{29}Si NMR of silicate sols prepared by acid-catalyzed hydrolysis and condensation of TEOS with $r \approx 1.5$ or 1.7 and fractal analysis of rheology data reveal that polysilicate species comprising spinnable sols are not simple rigid-rod ladder polymers or strictly linear polymers. Instead we observe a distribution of Q species consistent with the product of a statistical (random) growth process (suitably modified to take into account steric and inductive effects) and a mass fractal dimension $\gg 1$ indicating that rigid rods are not present on intermediate length scales (1–20 nm). The primary criterion for spinnability is high viscosity without premature gelation. This is accomplished by acid-catalyzed conditions employing low values of r, which produce extended rather than compact structures consistent with the conclusions of Sakka and coworkers based on rheological investigations. In order to achieve stable fibers a second criterion appears to be some additional condensation during fiber formation. This topic will be addressed in a future publication.

The technical assistance of D.A. Schneider and C.S. Ashley is gratefully acknowledged.

References

[1] A. Ziabicki, Fundamentals of Fiber Formation (Wiley, New York, 1976).
[2] M. Sacks and R. Sheu, J. Non-Cryst. Solids 92 (1987) 383.
[3] S. Sakka and K. Kamiya, J. Non-Cryst. Solids 48 (1982) 31.
[4] S. Sakka, in: Better Ceramics Through Chemistry, eds. C.J. Brinker, D.E. Clark and D.R. Ulrich (North-Holland, Amsterdam, 1984) p. 91.
[5] S. Sakka, K. Kamiya, K. Makita and Y. Yamamoto, J. Non-Cryst. Solids 63 (1984) 223.
[6] S. Sakka and H. Kozuka, J. Non-Cryst. Solids 100 (1988) 142.
[7] A. Einstein, Ann. Phys. 19 (1906) 289; 34 (1911) 591.
[8] Y. Abe and T. Misono, J. Polym. Sci. Polym. Chem. 21 (1983) 41.
[9] H. Tsuchida, Science of Polymers (in Japanese) (Baihukan, Tokyo, 1975) p. 85.
[10] S. Sakka, in: Sol–Gel Technology, Ed. L.C. Klein (Noyes, New Jersey, 1988) p. 140.
[11] S. Sakka, Y. Tanaka and T. Kokubo, J. Non-Cryst. Solids 82 (1986) 24.
[12] K. Kamiya, Y. Iwamoto, T. Yoko and S. Sakka, J. Non-Cryst. Solids 100 (1988) 195.
[13] R.A. Assink and B.D. Kay, J. Non-Cryst. Solids 99 (1988) 359.
[14] P.S. Belton, I.J. Cox and R.K. Harris, J. Chem. Soc. Faraday Trans. 2, 81 (1985) 63.
[15] B.D. Kay and R.A. Assink, J. Non-Cryst. Solids 104 (1988) 112.
[16] L.W. Kelts, N.J. Effinger and S.M. Melpolder, J. Non-Cryst. Solids 83 (1986) 353.
[17] C.A. Balfe and S.L. Martinez, in: Better Ceramics Through Chemistry II eds. C.J. Brinker, D.E. Clark and D.E. Ulrich (Mat. Soc. Boston, 1986) p. 27.
[18] B.D. Kay and R.A. Assink, ibid, ref. 17, p. 157.
[19] R.A. Assink, B.D. Kay and D.H. Doughty, J. Non-Cryst. Solids, to be submitted.
[20] D.W. Schaefer, MRS Bulletin 8 (1988) 22.
[21] D.W. Schaefer, J.E. Martin, A.J. Hurd and K.D. Keefer, in: Physics of Finely Divided Materials, eds. N. Boccaca and M. Daoud (Springer, Berlin, 1985) p. 31.
[22] C.J. Brinker, J. Non-Cryst. Solids 100 (1988) 31.
[23] H. Kozuka, H. Kuroki and S. Sakka, J. Non Cryst. Solids 100 (1988) 226.

2.3.5.2.2. Cluster–Cluster Growth Models

A second class of growth models is cluster–cluster aggregation [142]. (See Fig. 55.) These models describe growth that results when a "sea" of monomers undergoes random walks, forming a collection of clusters that continue to assemble by reacting with each other and with remaining monomers. Under diffusion-limited conditions (DLCA) clusters stick irreversibly on first contact. In reaction-limited conditions (RLCA) the sticking probability is less than unity. Compared to monomer–cluster aggregation, the more central screening of colliding clusters creates very open fractal structures even under reaction-limited conditions [121]. The fractal dimension for DLCA, 1.80 [142], is in fact only slightly less than for RLCA [134], 2.09, and both of the simulated structures in Fig. 55, in contrast to the monomer–cluster growth, cluster–cluster growth produces objects with no characteristic size.

[illegible] appears to pertain when there is not a con- [illegible] source of monomers and when there is no mechanism favoring condensation preferentially between low- and high-molecular-weight species. Reactions under [illegible] spectra shown in Fig. 33 shows that [illegible] conditions. At pH 1 the solution is [illegible] yet the concentration of Q^4 species is [illegible]. In fact the monomers are essentially [illegible]. Under strongly acidic conditions the [illegible] long before the gel point (see Fig. 29), which [illegible] condensation is low with respect to the rate of [illegible] depolymerization reaction is minimized. [illegible] of silica, condensation occurs by a [illegible] of silanol or alkoxide species.

[illegible] for large values of r, hydrolysis is [illegible]. Since all species are hydrolyzed, [illegible] dimers and other low-molecular-weight [illegible] the solution of monomers (e.g., a[illegible] involves the most basic silicate species, [illegible] or chains (Q^1). When monomers are [illegible] preferentially between Q^1 species and more [illegible] chain ends react with chain middles, leading to [illegible] structures. Because the rate of siloxane bond [illegible] reactions are suppressed, there are no [illegible] after the original source of monomers is [illegible]. Consequently, reaction-limited cluster–cluster [illegible] the early stage of the condensation process [illegible] for all examples ($D = 2.09$).

RLCA is also assured by two-step processes (see Table 2) in which the first step involves acid-catalyzed hydrolysis with understoichiometric additions of water ($r < 2$). Under these conditions, Assink and Kay [97] have shown that condensation commences before hydrolysis is complete. All the water is rapidly consumed to produce a distribution of partially hydrolyzed monomers which subsequently condense to form low-molecular-weight oligomeric species. (See Fig. 29.) Growth may cease when all available water and silanols are reacted. Addition of water plus catalyst (acid or base) in a second step ($r \geq 4$) causes all remaining alkoxide sites to hydrolyze, rendering all sites approximately equally reactive [24, 122]. Subsequent condensation is forced to occur primarily between oligomeric species (cluster–cluster growth). Porod slopes obtained for two-step acid- and two-step base-catalyzed silicates, -1.9 and -2.1, respectively [34,35], are consistent with the RLCA prediction of -2.09. (See Figs. 49 and 55.) This indicates that for the two-step base conditions employed ($r = 3.7$ and pH ~8) restructuring via dissolution-reprecipitation or redistribution is not sufficiently extensive prior to gelation to achieve primarily monomer–cluster growth conditions. However the more negative Porod slope, -2.1, obtained for two-step base conditions is consistent with more compact structures that do not swell upon dilution compared to two-step acid conditions ($P = -1.9$).

With regard to structural evolution, perhaps the most important feature of the acid-catalyzed growth mechanism is that for most oligomeric species condensation is virtually irreversible. Tenuous, fractal structures are therefore kinetically stabilized, because there is no mechanism for restructuring and there is little monomer available to fill in voids. Unlike base conditions in which dissolution-reprecipitation and the condensation process (monomer–cluster growth) naturally result in an "ordered" Q distribution (primarily Q^3 and Q^4 species), acidic conditions produce a distribution of Q^1–Q^4 species as expected for classic polycondensation of tetrafunctional monomers. (See Fig. 33.) The importance of irreversible condensation to the evolving silicate structures was predicted by Iler [1].

2.3.6. RHEOLOGICAL INVESTIGATIONS

Although rheological measurements characterize the bulk properties of a solution (for example, the viscosity or storage modulus), the dependence of rheological properties on concentration, molecular weight, or shear rate can be used to infer structural information on rather short [illegible] Qualitative rheological investigations have been performed on numerous sol-gel silicate systems. For example, the gel point is often identified by examination to be the time at which the solution loses fluidity, i.e., it no [illegible]

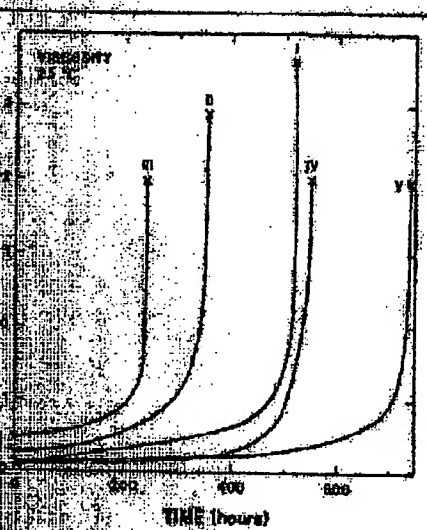

[illegible] viscosity for acid- or base-catalyzed TEOS systems. [illegible] Samples I–V are identified in Table 17.

[illegible] gel in container is tipped [143]. Numerous quantita- [illegible] have also been performed during the course of [illegible] [144]. In these investigations, the gel point [illegible] at which the viscosity is observed to increase [illegible] viscosity versus time measurements are used to [illegible] required to draw fibers or thin sheets directly [illegible] Sakka and coworkers [28,31] reported that fiber [illegible] the viscosity was ~1–100 Pa-s [29], and sheet [illegible] was ~1–10 Pa-s. However, accord- [illegible] most of the measured viscosities were not [illegible] viscometers were not used and, hence, shear

[illegible] acid- and base-catalyzed silicate systems in [illegible] were varied as indicated in Table [illegible] compositions 1 and 2) are suitable for [illegible] [illegible] is suitable for bulk gels, and the [illegible] composition 4 ($r = 20$), results in the forma- [illegible] viscosity versus shear rate measurements

Table 16.

Compositions Investigated by Sacks and Sheu [145].

Solution	Water/TEOS Molar Ratio, r	Ethanol/TEOS Molar Ratio	Catalyst/TEOS Molar Ratio	Aging Temperature
1	2	3.8	0.1 HNO_3	25°C
2	4.5	1.91	0.0027 HNO_3	25°C
3	20	0.3	0.01 HNO_3	25°C
4	20	3.82	0.01 NH_4OH	50°C

for composition 1 show Newtonian flow behavior (shear-rate-independent viscosity) for aging times up to 1176 h. This is followed by a period of shear-thinning behavior (viscosity decreases with increasing shear rate). Further aging results in yield behavior and hysteresis in the shear stress versus shear rate curve indicating thixotropic flow behavior.

These changes are similar to those observed in marginally stable particle-liquid systems as the volume fraction of particles is increased [146]. At low particle concentrations the viscosity is rather unaffected by particle–particle interactions and Newtonian behavior is observed. Aging leads to aggregated structures, causing the viscosity to increase due to liquid immobilized within the aggregate, which in effect increases the apparent solids loading. As the shear rate is increased, these tenuous aggregates break down, releasing immobilized liquid and thus reducing the viscosity. This corresponds to shear-thinning behavior. Further aging leads to extensive network formation imparting elastic character to the system as indicated by the yield stress in the shear stress versus shear rate curve. After the yield stress is exceeded shear-thinning behavior and hysteresis are observed (thixotropic flow behavior).

Spinnability (the ability to draw fibers from the solution) was observed for compositions 1 and 2 but not for compositions 3 and 4 in Table 16 [145]. The best spinnability was observed when the viscosity behavior was highly shear thinning but not thixotropic. Shear-thinning behavior however is not sufficient for spinnability. All systems exhibited transformations from Newtonian to shear-thinning to gel behavior. Compositions 1 and 2 are distinguished from compositions 3 and 4 in that their viscosities were not higher when the transformation to shear-thinning behavior occurred. Apparently a very high viscosity is necessary to prevent the drawn fiber from breaking up into droplets. High viscosities required for stable fiber formation are generally achieved by concentration of the sol through solvent evaporation [31].

Sakka and coworkers [28,29,31,146] and Kamiya *et al.* [147] have investigated the rheology of silicate systems prepared from TEOS (see Table 17) in conjunction with fiber formation (spinnability). Acid- and

Table 17.

Compositions and Behavior of Sol-Gel Systems Investigated by Sakka *et al.* [28,29,51]

Solution	$Si(OC_2H_5)_4$ (g)	H_2O (g)	C_2H_5OH (g)	Mole Ratio (r) of H_2O to $Si(OC_2H_5)_4$	Catalyst[a]	Time for Gelling (h)	Stability
I	169.3	14.7	239.7	1	HCl	125	stable
II	182.0	15.9	83.4	1	HCl	360	stable
III	169.3	282.6	37.5	20	HCl	288	stable
IV	50	3.8	47.6	1	NH_4OH	566	stable
V	50	7.5	47.6	2	NH_4OH	240	stable

[a] Mole ratio of HCl or NH_4OH to the $Si(OC_2H_5)_4$ is 0.01.

base-catalyzed systems prepared with r values ranging from 1 to 20 were evaluated by determining the concentration-dependence of the reduced viscosity, η_{sp}/C, and the molecular-weight-dependence of the intrinsic viscosity, $[\eta]$. Figure 60 compares the concentration dependence of η_{sp}/C for composition I (acid-catalyzed, $r = 1$, see Table 17) to that of LUDOX® (spherical silicate colloids) and sodium metasilicate (chain-like silicates) after various periods of aging in open containers. The reduced viscosity of a solution of noninteracting spherical particles (e.g., LUDOX®) is independent of concentration, C [148]:

$$\eta_{sp}/C = k/\rho \tag{57}$$

where k is a constant and ρ is the density of the particles. Therefore the silicate species present at $t/t_{gel} = 0.34$ (see Fig. 60) are inferred to be compact and noninteracting. This is consistent with the Newtonian behavior observed by Sacks and Sheu [145] at early stages of aging.

Further aging causes a progressively larger dependence of η_{sp} on C. According to the Huggins equation, chainlike or linear polymers (e.g., metasilicate) show a concentration-dependence of the reduced viscosity [149]:

$$\eta_{sp}/C = [\eta] + k[\eta]^2 C \tag{58}$$

where $[\eta]$ is the intrinsic viscosity and k is a proportionality constant. Therefore the more readily larger dependence of η_{sp}/C on C with aging time (Fig. 60) may be explained as arising from a gradual progression of the silicate species from small, noninteracting species to extended, weakly branched polymers. This corresponds to the shear thinning region observed by Sacks and Sheu [145].

Figure 61 plots intrinsic viscosity versus log number-averaged molecular weight, M_n, for the base-catalyzed silicate systems in which r was varied from 1 to 20.

Fig. 60.

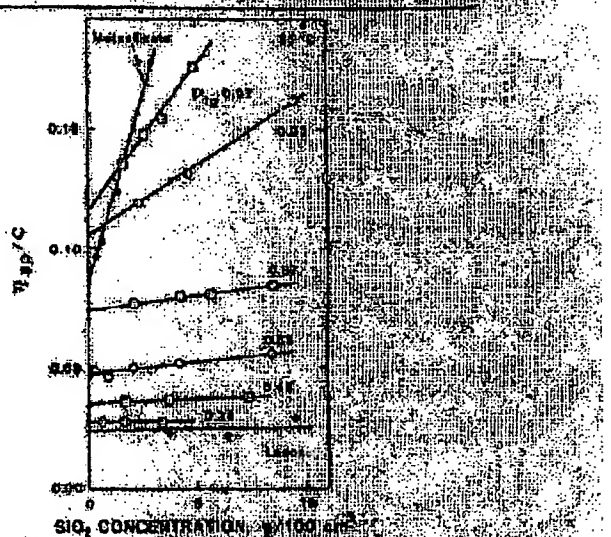

Concentration-dependence of the reduced viscosity, η_{sp}/C, of silica sols prepared from TEOS, $r = 1$, see Table 17) as a function of t/t_{gel}. Comparative data for LUDOX® and sodium metasilicate are shown for comparison [51].

For organic polymer solutions it is known that $[\eta]$ is related to M_n according to [32]:

$$[\eta] = kM_n^{\alpha} \tag{59}$$

where k is a constant that depends on the kind of polymer, solvent, and temperature, while α depends on the polymer structure: $\alpha = 0$ for rigid, spherical particles; $\alpha = 0.5$–1.0 for flexible, chainlike, or linear polymers; and $\alpha = 1.0$–2.0 for rigid, rodlike polymers [31]. For example, for high molecular-weight polymethylsiloxanes, $\alpha = 0.5$ for linear polymers, $\alpha = 0.21$–0.28 for branched polymers, and $\alpha = 0.3$ for spherical particles [149]. From this relationship the results presented in Fig. 61 indicate that the spinnable systems ($r = 1$ or 2) are composed of flexible chainlike or linear polymers ($\alpha = 0.64$–0.75), whereas the nonspinnable systems are composed of more highly branched structures. Based on fractal geometry, Eq. 59 may be re-expressed as follows [122]:

$$\eta = R_g^3/M_n = M_n^{(2/d_f)-1} \tag{60}$$

Fig. 61.

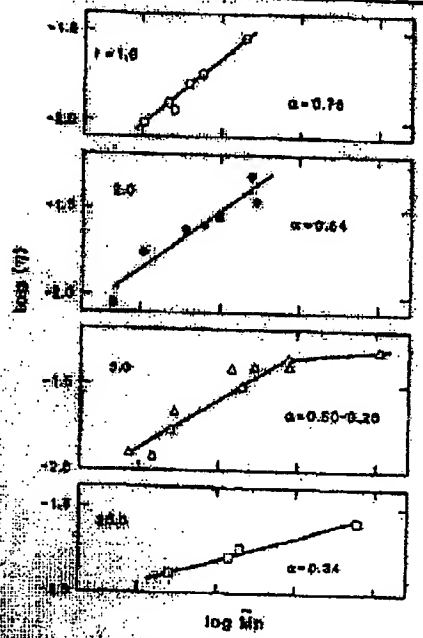

Log [intrinsic viscosity] versus log number average molecular weight, M_n, for solutions of linear polymers prepared by acid-catalyzed hydrolysis of TEOS and r = 1–20 [28]. α = slope = a in Eq. (6).

where R_g is the radius of gyration and d_f is the mass fractal dimension. According to Eq. (6) (see Eq. 5) α is equivalent to $(3/d_f - 1)$. Therefore α values of 0.64–0.75, measured for extrudable systems correspond to mass fractal dimensions d_f = 1.82 to 1.71, consistent with structures ranging from linear, weakly branched polymers to moderately branched polymers (Table 15). It is not possible to distinguish among these various structures on the basis of d_f alone.

Combining the results of Sakka and coworkers [28,29,31,146] to those of Scherer and Hdach [151], we see that a consistent set of requirements for spinnable gels emerges: slow gelation, acid catalyst, and low concentration. High viscosity kinetically stabilizes the fibers from [illegible] Eqs. (5)–(6), for any particular concentration

and extent of condensation, weakly branched "extended" structures, e.g., chains or rods ($d_f \ll 3$), are more efficient than compact structures, e.g., uniform particles ($d_f = 3$), in increasing the viscosity. Overlapped extended structures interact at lower concentrations which explains the concentration- and molecular weight-dependence of the reduced and intrinsic viscosities, respectively. As we have discussed in Section 3.6.3, acid-catalyzed conditions lead to the formation of weakly branched, extended structures that exhibit a strong concentration dependence of R_g, suggesting significant overlap prior to gelation. The combination of acid-catalyzed conditions and low values of r allows the concentration (and therefore viscosity) to be greatly increased by solvent evaporation without premature gelation, both because the condensation rate is low under acidic conditions and because many ethoxide groups are retained on the siloxane backbone, further reducing the condensation rate. Further solvent evaporation, just as one does when drawing precursor fibers, causes a sufficient increase in viscosity to stabilize the drawn fiber due to the strong concentration-dependence of viscosity.

In order to determine if linear or rigid-rod polymers are necessary for spinnability, Sakka *et al.* investigated the hydrolysis and condensation of difunctional, dimethyldiethoxysilane and trifunctional, phenyltriethoxysilane [150]. These molecules are potential precursors for linear and ladder polymers, respectively. It was observed that the hydrolysis of dimethyldiethoxysilane resulted preferentially in the formation of cyclic oligomers leading to immiscibility. Based on this observation, it was concluded that rigid-rod (e.g., ladder) polymers are necessary for fiber formation because flexible, linear polymers would tend to cyclize [150] leading to compact structures. Ladder polymers have also been associated with the inflection in the viscosity-versus-time behavior observed in some base-catalyzed systems and with the theoretical quantity of water required to form ladder polymers, r = 1.7. (See Fig. 62.)

Several factors argue against the existence of rigid-rod ladder polymers in spinnable systems, however. First, according to Eqs. (5) and (6), rigid-rod polymers should have a mass fractal dimension d_f = 1, resulting in an α value of 2 rather than 0.75 or 0.64 as observed (Fig. 61). Second, solutions containing rigid-rod polymers should exhibit Porod scattering, $I \propto q^{-4}$. Preliminary SAXS experiments show that the spinnable systems are highly polydisperse [151]: no power law region is observed, which implies that if rigid-rod polymers are present, they do not constitute the predominant solution species. Finally, it is unlikely that random growth of tetrafunctional precursors results in such highly ordered species as ladder polymers.

The general synthetic approach to the formation of ladder polymers is acid-catalyzed hydrolysis of trifunctional silanes (e.g., trichlorophenylsilane)

This Page is Inserted by IFW Indexing and Scanning Operations and is not part of the Official Record

BEST AVAILABLE IMAGES

Defective images within this document are accurate representations of the original documents submitted by the applicant.

Defects in the images include but are not limited to the items checked:

- ☐ BLACK BORDERS
- ☐ IMAGE CUT OFF AT TOP, BOTTOM OR SIDES
- ☐ FADED TEXT OR DRAWING
- ☑ BLURRED OR ILLEGIBLE TEXT OR DRAWING
- ☐ SKEWED/SLANTED IMAGES
- ☐ COLOR OR BLACK AND WHITE PHOTOGRAPHS
- ☐ GRAY SCALE DOCUMENTS
- ☐ LINES OR MARKS ON ORIGINAL DOCUMENT
- ☐ REFERENCE(S) OR EXHIBIT(S) SUBMITTED ARE POOR QUALITY
- ☐ OTHER: _____

IMAGES ARE BEST AVAILABLE COPY.
As rescanning these documents will not correct the image problems checked, please do not report these problems to the IFW Image Problem Mailbox.